Assessment of Spatio-Temporal Dynamics of Drought Stress Anomalies Using Hyperspectral Imagery Fusion

Pragyi Choudhary[1], Rajesh Dhumal[1], Soumyashree Kar [2*]

[1] Symbiosis Institute of Geoinformatics,
5th and 6th Floor, Atur Centre, Gokhale Rd, Model Colony, Shivajinagar, Pune, Maharashtra, 411016, India

[2*] Centre of Studies in Resources Engineering (CSRE),
Indian Institute of Technology Bombay (IIT BOMBAY),
Powai, Mumbai, Maharashtra 400076, India

KEYWORDS: Drought stress anomalies, Hyperspectral, Sentinel-2 MSI, Vegetation indices, Spatio-temporal trend analysis, Spectral anomaly detection.

ABSTRACT

Drought stress generates considerable ecological and physiological effects, endangering vegetation health, forest resistance, and the management of water resources. In this study, the combination of hyperspectral (AVIRIS Classic, 2013–2018) and multispectral (Sentinel-2, 2019–2025) imagery was utilized to evaluate the spatio-temporal dynamics of drought in California's ecologically fragile Sierra Nevada region. In order to overcome the spectral limitation of multispectral data, a solid methodology based on an Analytic Hierarchy Process (AHP) framework was established. This method algorithmically weighted and combined eight spectral indices according to their biophysical correspondence with drought, with greatest weight on Moisture Stress Index (MSI), then Normalized Difference Drought Index (NDDI) and Normalised Burn Ratio (NBR), in order to produce a composite drought severity rating. This rating was classified with a Random Forest model with high accuracy with an overall accuracy of 86.53% and balanced accuracy of 86.37%. Our analysis between 2013 and 2025 indicates varied but strengthening trends of drought with an increased escalation in the spatial magnitude and severity of exceptional drought (D4) conditions, especially for southern areas since 2019. The 2026 forecast shows an increased deterioration in drought conditions. This paper shows how multi-sensor integration, with the help of a decision-theoretic weighing scheme is a very powerful, scalable, and transferable paradigm of reliable drought monitoring, offering valuable information to anticipatory resource management and mitigation plans in mountain-like drought-prone areas around the world.

1.INTRODUCTION

The assessment of spatio-temporal drought is essential to comprehend and investigate the vegetation and ecosystem susceptibility of a region on a time basis. Hydrological extremes and vegetation stress are directly impacted by rapidly shifting and evolving weather patterns and ecosystem conditions. The impacts of droughts on our natural ecosystems can be huge and far extending, as well as the socioeconomic activities they disrupt.

The mountain ranges Sierra Nevada are the most ecologically and hydrologically important areas in California. Although it is a hydrology-prone area, it is the main source of water in the state and at the same time experiences unprecedented environmental stress due to droughts caused by climate change. This paper relies on edge-cutting remote sensing technology and advanced analytical procedures to investigate vegetation drought responses to the different elevation gradients in the central and southern Sierra Nevada forests. The present study examines the most recent data, which is the most important one and spans the years 2013-2025. The significant point in the analysis is the ecologically sensitive period of snowmelt/peak dryness transition when the vegetation is especially prone to moisture shortage. The research fills a number of inherent knowledge gaps in the interpretation of ecosystems susceptibility to the long-term drought conditions via an unprecedented fusion of hyperspectral and multispectral remote sensory datasets.

SIGNIFICANCE OF THE STUDY:

Climate change scenarios such as the upsurge in frequency and severity of drought events has led to an immediate demand on more advanced monitoring and assessment instruments. The devastating loss of more than 100 million trees in the 2012-2016 drought period is the result of the Sierra Nevada ecological crisis (Young et al., 2017). This disaster determined the necessity of examining and creating sophisticated drought detection techniques.

The research makes significant contributions through implementing a dual-sensor approach combining AVIRIS Classic hyperspectral and Sentinel-2 multispectral data for the years 2013-2018 and 2019-2025 respectively which overcomes the traditional limitations of single-sensor systems by leveraging their complementary strengths and conducting a temporal analysis. The AVIRIS sensor provides accurate narrow band spectral resolution (224 bands) for fine stress detection, whereas Sentinel-2 provides better temporal cover for observing drought evolution. The research entails the use of Level 2 AVIRIS hyperspectral products to reduce processing while still achieving accuracy. The study allows an effective, large-scale characterization of vegetation stress throughout California's Sierra Nevada, a vital water source with rising drought concerns, by avoiding complex preprocessing processes. Creation of drought vulnerability maps, reveal how different vegetation zones respond to water stress across the Sierra Nevada's dramatic elevational gradient . These maps locate the most sensitive regions to be given high priority in

conservation. Confirmation of best spectral indices, which are essential for stress detection at the critical season shift from snowmelt to peak dryness, assists in effective strategic planning. Considering the pace of climate change that is occurring these developments will be essential in ensuring the water security of California as well as the ecological integrity of its forest habitats.

1.1.OBJECTIVES OF STUDY:

The current drought monitoring capabilities contain certain critical gaps. This study is designed to achieve the following four primary research objectives:

1. To design and test an autonomous AHP-ML procedure for long-term mountainous region drought monitoring by fusing multi-sensor spectral indicators using an Analytic Hierarchy Process (AHP) and severity classification with an optimized Random Forest framework.

2. To examine the patterns of spatio-temporal severity of drought by using the derived workflow to produce annual maps of drought classification (D0-D4), estimating the development of trends through time and elevation gradients.

3. To critically assess and confirm the efficiency of spectral indices in detecting drought by orderly comparing the performance of each, measuring the class-specific metrics of accuracy and finding the best thresholds of severity level classification.

1.2.PROBLEM STATEMENT:

Current drought monitoring methods address three fundamental limitations:

1. Temporal Gaps in Coverage: The vast majority of current studies deal with one drought or short periods, without the decade-long perspective to decipher long-term trends as well as responses from the ecosystem. Our twelve-year study (2013-2025) offers unprecedented temporal perspective.

2. Spectral Constraints: Traditional multispectral systems (e.g., MODIS, Landsat) do not possess the bandpass resolution to capture weak physiological indicators of stress that can be observed with hyperspectral sensors. The current work shows that hyperspectral imagery discloses patterns undetectable with multispectral systems.

3. Methodological Inconsistency: In spite of the progression in remote sensing, there exists a significant gap in terms of availability of standard, thoroughly tested hyperspectral processing protocols specifically tailored for mountainous terrain. These protocols are needed in order to properly combat issues such as cross-sensor calibration, intricate topographic correction, and the merging of climatic data in order to obtain strong spatio-temporal trend analysis.

2.LITERATURE REVIEW

2.1.PREVIOUS WORKS:

Remote sensing techniques have been implemented using hyperspectral and multispectral data frequently, to detect drought stress in forest stands because of their ability to identify subtle vegetation anomalies. Because of its high spectral resolution, hyperspectral data are more effective than conventional multispectral data in detecting early signs of physiological vegetation stress like alterations in chlorophyll content, leaf wetness, and structural modifications (Ahmad et al., 2021).

Ahmad et al. (2021) proved the efficacy of AVIRIS-NG hyperspectral imaging in India's forest classification at the species level with an accuracy estimation of 80%. Their study laid the basis on which narrow-band sensors can identify subtle biochemical features necessary for early drought detection. Likewise, Hati et al. (2021) employed AVIRIS-NG to map vegetation stress in mangroves by calculating nine hyperspectral indices, such as NDII and PRI, sensitive to pigments and moisture. This shows the usability of spectral indices in ecological stress monitoring, especially in forest ecosystems.

Previous studies such as C.J. et al., (2019) successfully employed AVIRIS hyperspectral imagery for detecting drought-induced tree mortality in the Sierra Nevada using classification techniques like SAM and MNF-based dimensionality reduction, their temporal focus was limited to post-2012 drought years. This research expands the time frame to a longer window period (2013–2025), includes multispectral Sentinel-2 imagery for wider comparison, uses vegetation indices to identify stress anomalies prior to mortality, and adds climatic indices (SPI, PDSI) for relating biophysical response to meteorological drivers.

Loggenberg et al. (2018) used ground hyperspectral imaging and machine learning classifiers like Random Forest and XGBoost to distinguish water-stressed and healthy vines in viticulture. The findings highlighted that full-spectrum models could classify early-developing drought stress well, and spectral smoothing sometimes decreased classification accuracy—a consideration to remember while conducting AVIRIS data pre-processing.

In Sierra Nevada, other environmental studies indicate long-term consequences of drought on forest conditions and tree mortality. Fettig et al. (2018) linked the reason for widespread tree mortality with the 2012–2016 southern and central Sierra Nevada drought, of which Pinus ponderosa was the most affected species. Their observations underscore the value of pre-emptively identifying such effects using remote sensing technology. Pile et al. (2019) extended this finding by examining how drought had interacted with pests and fire suppression to cause forest decline. These drivers have the potential to be mapped using hyperspectral stress indices.

Hydrologically, Hatchett and McEvoy (2018) first employed *snow drought* to characterize the Sierra Nevada conditions of diminished snowpack but not necessarily diminished precipitation. The term is particularly apt for your research, as it exposes the dry, transitional phase after snowmelt to the detection of vegetation stress. A question is also posed regarding the validity of linking snowpack variability to drought analysis with spectral indicators.

Crockett and Westerling (2018) described the climatic setting of stress, outlining how high vapor pressure deficit (VPD) and high temperature escalated fire and drought severity. Remote sensing predictors are characterized by moisture indexes (NDMI, NDWI) and chlorophyll-related indexes (PRI, MCARI) derived from AVIRIS Classic data.

Lastly, Zhao and Running (2016) simulated global drought effects on net primary productivity from coarse satellite data, noting that drought strongly suppresses biomass production.Such production fluctuation can be measured at greater resolutions through hyperspectral data, which is one of the elements of forest resource planning.

Recent researches have established that hyperspectral remote sensing, i.e. AVIRIS-like data, can provide precise data on stress associated with drought in diverse ecosystems.

However, temporal limitation, poor revisit frequency, and complex processing pipeline have hindered large-scale applications. This study addresses such limitations by integrating multi-year hyperspectral (AVIRIS Classic) and multispectral (Sentinel-2 MSI) data sets for evaluating temporal anomalies and classification accuracy, once again standardizing a comparative pipeline for drought monitoring in mountain forest ecosystems.

2.2.IMPORTANCE OF THE STUDY:

This study makes major contributions to drought monitoring science by presenting a new, scalable methodology for measuring vegetation stress with high accuracy.

Scientific Contributions:

This research's main scientific contribution is the creation of an AHP-Random Forest framework that successfully integrates hyperspectral and multispectral data for strong drought severity classification. Through the utilization of AVIRIS's high spectral resolution to define accurate baselines and Sentinel-2's high temporal resolution for ongoing observation, this research illustrates a mechanism by which to transcend the intrinsic limitations of single-sensor systems. The AHP weighting scheme mathematically formalizes the fusion of multiple spectral indices according to their documented biophysical relationships with drought, going beyond ad-hoc combinations of indices. This methodology resulted in a very accurate and interpretable model (total accuracy: 86.53%) to map drought severity (D0-D4) with empirical confirmation of elevation-dependent trends in drought vulnerability, specifically the sensitivity at mid-elevation conifer forests.

Technological Innovation:

This study generates novel processing streams for hyperspectral time series analysis and assists in integrating and incorporating multi-sensor capabilities to improve workflow, analysis and management. It also employs advanced machine learning techniques specially designed for environmental remote sensing.

Practical Applications:

Practical Applications involve aiding California's Forest Carbon Plan through the delivery of accurate drought impact analysis, aiding water resource planners in designing drought contingency plans, improves wildfire hazard appraisal through advanced vegetation stress monitoring, directs conservation prioritization in endangered ecosystems and research required for early monitoring and monitoring of droughts making it simple to develop early warning systems and become resilient

Strategic Planning and Policy- Making:

The research provides climate adaptation planning supported by scientific evidence, enables decision-making in the allocation of water and contributes to the development of forest management policies. The integrated approach developed through this work provides an exportable template for tracking climate-sensitive ecosystems globally, especially in snow-dependent mountain ecosystems experiencing similar hydroclimatic change. Our research has direct utility for resource managers while pushing the science forward on the effects of drought in montane ecosystems

3.STUDY AREA

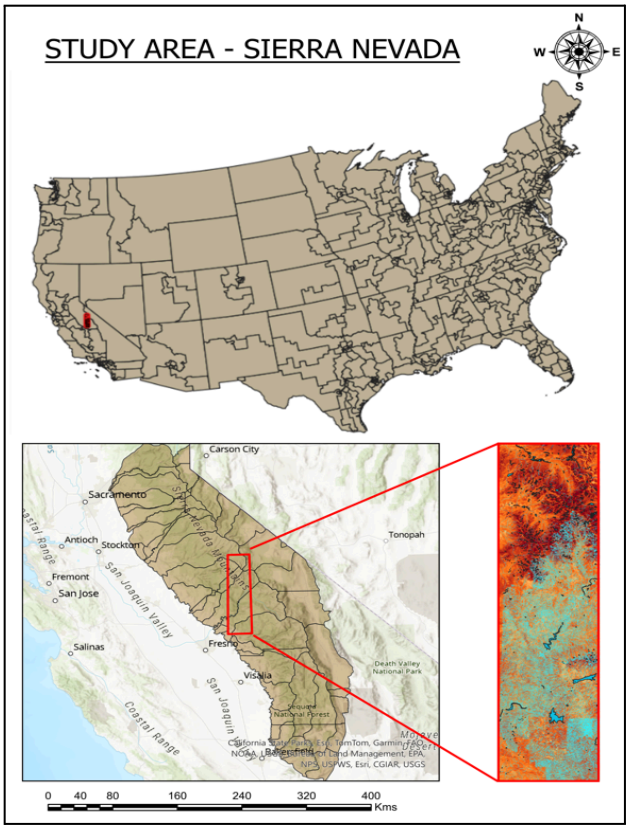

Figure 1. Sierra Nevada – Study Area

3.1.STUDY AREA – GENERAL DISCUSSION:

During the last 20 years, the central and southern Sierra Nevada of California, USA, has suffered more serious drought conditions and is thus a place of environmental diversity and utmost significance (Diffenbaugh et al., 2015). The region is located between 36°55'55.54\"N, 119°28'17.33\"W in the southwest and 37°55'41.13\"N, 119°09'52.44\"W in the northeast with an elevation gradient of about 500 meters (foothills) to over 4,000 meters (high alpine region) in width (Millar et al., 2022). At the lowest level, the site has drought-tolerant chaparral and oak woodlands, at mid-level mixed-conifer forests with Ponderosa pine (Pinus ponderosa) and white fir (Abies concolor), and at the highest elevation, sensitive whitebark pine (Pinus albicaulis) (Fettig et al., 2019).

The snowpack is the foundation of the hydrological health of the Sierra Nevada, which is essential both to human populations and the natural ecosystems because it is the major watershed in California and generates about 60 percent of the freshwater in the state (Hatchett et al., 2018). The region has recently been of interest in research on the effects of climate change that has had an unprecedented high rate of tree loss, particularly as a result of the moisture stress and bark beetle infestations together.(Asner et al., 2016). A dramatic change in fire regimes can be seen from recent research, which indicates that the proportion of high-severity wildfires has risen from below 10% of area burned during previous decades to more than 40% during recent decades (Steel et al., 2023). These alterations are the result of a century of fire suppression policies that have changed fuel loads and forest structure, combined with climate change and extended drought conditions (Stephens et al., 2021).

3.2.STUDY AREA – RESEARCH ORIENTED

The central and southern parts of Sierra Nevada were chosen for this study because of its high climatic sensitivity and well-established vegetation responses to water scarcity. The area is a perfect natural setting for using remote sensing to analyze the effects of drought during the transitional month from snowmelt to peak summer dryness, which helps in understanding and planning early warning systems . This temporal focus captures vegetation at its most vulnerable stage, when water availability shifts dramatically and stress signals become most apparent in spectral data.

The analysis shows that the elevational gradient of Sierra Nevada produces discrete vegetation zones that react to drought in different ways.
While mid-elevation conifer forests (1,500–2,500 m) display combined drought and pest damage signatures in their spectral profiles, lower elevation chaparral and oak woodlands (500–1,500 m) show rapid moisture stress in June NDWI values. The most sensitive climate change indicators are found at the highest elevations (>2,500 m), where whitebark pine predominates. June spectral indices show increasingly earlier seasonal stress patterns.
Comparative evaluation of drought resilience across ecosystems is made possible by these elevational variations.

The region's hydrology further enhances its research value. June snowmelt patterns, visible in satellite imagery, directly influence summer water availability. Areas with early snowpack depletion exhibit corresponding early stress signals in vegetation indices, which frequently predict future wildfire risk. The drought years 2012–2016 offer a particularly useful reference, since June AVIRIS data document acute stress reactions that occur before widespread tree death.

Detailed monitoring of these dynamics is made possible by the combination of multispectral (Sentinel-2) and hyperspectral (AVIRIS) data. June is the best month to capture inter annual variability in the transition month, as it records both the tail end of snowmelt and the head end of summer drought stress. Sierra Nevada temporal resolution and elevational diversity are combined to offer an effective platform in the comprehension of vegetation vulnerability and drought generation in Mediterranean-mountain systems. The temporal resolution and the elevational diversity of Sierra Nevada are applied integrally to offer an effective platform for the comprehension of vegetation vulnerability and drought progression in Mediterranean-mountain systems. The clear spectral contrasts between healthy and stressed vegetation in June, as well as the region's well-documented climate history, make the region especially amenable to the development and verification of remote sensing techniques for detecting drought.

3.3.CHARACTERISTICS OF THE STUDY AREA

The location of the study is a subset of the central and southern Sierra Nevada between 3655 and 3755N latitude that has an unusually promising natural study site because of its unusual mix of features:

High altitude Gradients: The research site has an astonishing 3,500m of vertical range (500-4,000m) supporting vegetation zones that have varying drought susceptibility.

Drought-resistant chaparral and oak woodlands dominate low altitudes (500-1,500m) and mixed-conifer forests with species such Ponderosa pine and white fir were strongly affected by the occurrence of severe droughts in the recent past. Whereas the areas with elevation (>2,500m) are rich in subalpine climate-sensitive species, such as whitebark pine.

Snowpack dependent hydrology: Snowpack in Sierra Nevada is a large natural storage of the winter precipitation which is released slowly in the spring and summer. Hydrologic health of the region is critical to the agriculture sector and millions of people in the state because approximately 60 percent of Californian freshwater runs off of this snowmelt.

Climate Change Hotspot: The region has one of the most dramatic climate change effects in the entire North American continent with a rise nearly 2 times the global average amount of snowpack loss since the 1950s, a 2-3 weeks earlier spring snowmelt than the historical pattern, and an augmentation of vapour pressure deficit (VPD) leading to drought stress.

Ecological crisis epicenter: The area was the epicenter of the recent ecological disasters that hit California, such as the 2012-2016 drought, which caused the massive mortality of trees, the outbreak of bark beetles due to the drought stress, and the prevalence and severity of wildfires have risen to unprecedented levels.

Global applicability: Sierra Nevada is a perfect study area to examine the Mediterranean-mountain ecosystems in the globe that are experiencing similar climatic stresses so that our results can be widely applicable to other endangered regions.

4. METHODOLOGY

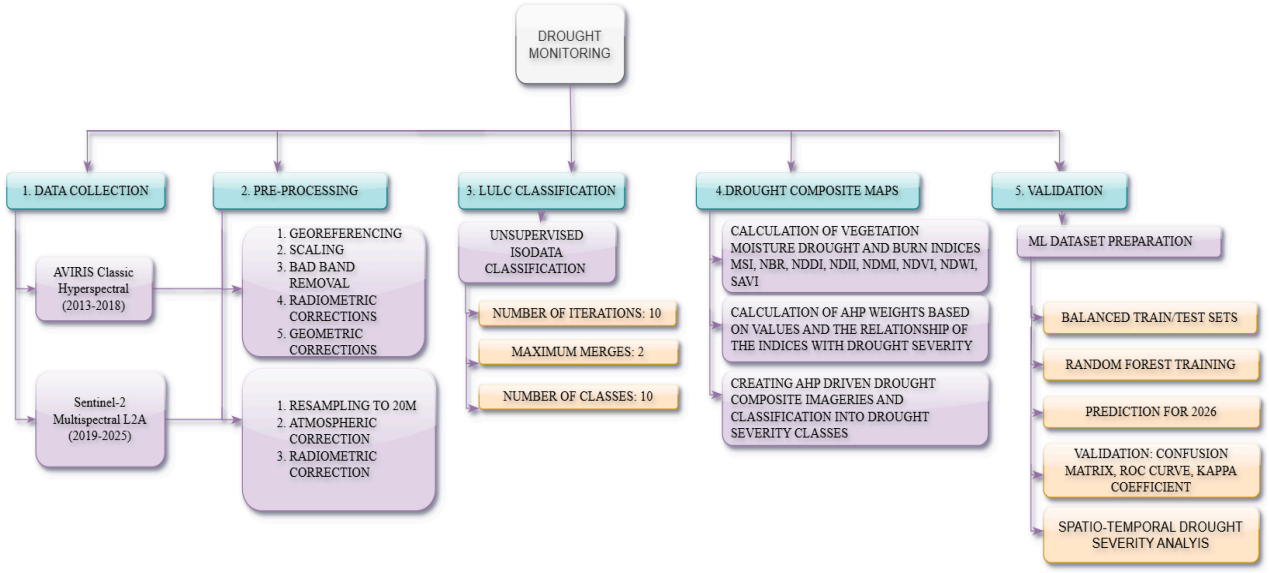

4.1.DATA ACQUISITION AND SOURCES

The analysis used high-resolution hyperspectral and multispectral satellite data, and regional scale climate data to evaluate and detect drought patterns in Sierra Nevada in the year 2013 to 2025. There were two major remote sensing platforms used:

AVIRIS Classic Level 2 Data (2013–2018):
NASA EarthData provided reflectance imagery of the atmosphere that had been orthorectified and atmospherically corrected. The AVIRIS sensor provides a high level of hyperspectral data in 224 narrow bands, which measures fine-scale physiological changes in vegetation.

Sentinel-2 MSI Level-2A Data (2019–2025): Multispectral imagery was obtained from the Copernicus Open Access Hub. The Level-2A product is atmospherically corrected using the Sen2Cor processor and includes scene classification and cloud masks. This data is critical for temporal continuity beyond the AVIRIS acquisition window.

PRISM DATA: Data on climate was obtained via the PRISM Climate Group, Oregon State University, at 4 km of spatial resolution and it was used to calculate standardized drought indices as follows: month precipitation, minimum and maximum temperature, mean temperature, and vapor pressure deficit (VPD). Data was extracted for the month of June each year to capture peak drought seasonality.

4.2.HYPERSPECTRAL IMAGE PRE- PROCESSING (AVIRIS Classic) IN ENVI 5.0:

AVIRIS Level 2 products are pre-corrected for atmospheric and geometric distortions, extensive preprocessing is not required. Although there are several crucial steps that still need to be followed to prepare the data for analysis and ensure compatibility with other datasets:

Bad Band Removal: Bands affected by strong water vapor absorption and sensor noise were systematically excluded. Specifically, bands 1–5, 104–114, 148–178, and 221–224 were removed based on the spectral profile and quality flags.

Reflectance Scaling: AVIRIS Level 2 data is delivered with

reflectance values scaled by a factor of 10,000. To convert these to standard reflectance units (ranging from 0 to 1), each band was divided by 10,000 using Band Math in ENVI.

SCALING = float(bi) / 10000.00

Where, i = band number / a set of bands in a dataset

Spectral Subsetting: Diagnostic wavelengths relevant to vegetation and moisture content were retained. This included the visible (500–750 nm), near-infrared (750–1000 nm), and shortwave infrared regions (1500–2300 nm).

MNF Transformation: The Minimum Noise Fraction (MNF) transformation was performed to separate noise from signal and reduce dimensionality. The first 20 MNF bands, accounting for the majority of variance, were retained for further analysis.

4.3.MULTISPECTRAL IMAGE PRE- PROCESSING (Sentinel- 2 L2A):

Sentinel-2 L2A images were processed with minimal effort due to their pre-processed nature. The following steps ensured uniformity with AVIRIS data:Spatial sampling:

Sentinel-2 bands available at 20m resolution were chosen to ensure spatial consistency with hyperspectral products.

Binary Scaling: Binary reflectance scaling was also done for sentinel 2 products where values were similarly scaled by a factor of 10,000 so that both hyperspectral and multispectral products have the same scaling.

Spatial Subsetting: A region of interest (ROI) shapefile for the Southern Sierra Nevada was created to spatially constrain both Sentinel-2 and AVIRIS images using ENVI's spatial subset tool.

4.4.DATA HARMONIZATION AND CROSS SENSOR VALIDATION:

Maintaining consistency between the discrete AVIRIS (2013-2018) and Sentinel-2 (2019-2025) datasets was important to support strong temporal analysis. Since there was no overlap in time between the two sensor acquisition periods, harmonization came about through a three-step procedure centered on the derived indices instead of raw reflectance data. To begin, all Sentinel-2 bands were resampled to a uniform 20m spatial resolution to correspond with the AVIRIS processed data. Second, reflectance values of both sensors were normalized to a shared 0-1 range. Third, the most important vegetation and moisture indices (NDWI, NDMI, MSI, NDVI, SAVI, NDII, NDDI, NBR) were computed for each sensor with their respective bandpass definitions. This method produced a homogenous, comparable time series of biophysical indicators allowing the effortless joining of both datasets into an integrated drought monitoring system.

4.5.VEGETATION, MOISTURE AND DROUGHT INDICES COMPUTATION:

Vegetation and Moisture and Drought Indices Computation: Vegetation and water stress indices were computed using Band Math in ENVI 5.0.

Table 1: showing calculated indices and their formulas

Index	Formula	Description	References
NDVI	(NIR - Red) / (NIR + Red)	Vegetation greenness	Tucker et al. (1979)
NDWI	(NIR - SWIR) / (NIR + SWIR)	Vegetation water content	Gao et al. (1996)
NDMI	(NIR - SWIR1) / (NIR + SWIR1)	Moisture content	Wilson et al. (2002)
NDII	(NIR - SWIR2) / (NIR + SWIR2)	Canopy water stress	Hardisky et al. (1983)
NBR	(NIR - SWIR2) / (NIR + SWIR2)	Burn severity /dryness	Key et al. (2006)
NDDI	(NDVI - NDWI) / (NDVI + NDWI)	Drought stress	Gu et al. (2007)
MSI	SWIR / NIR	Moisture stress index	Hunt et al. (1989)
SAVI	((NIR - Red) / (NIR + Red + L)) * (1 + L), L=0.5	Soil-adjusted vegetation	Huete et al. (1988)

4.6.PRISM DATA PROCESSING:

The datasets were integrated with long-term meteorological data to investigate how climate factors impact vegetation stress across the Sierra Nevada from 2013 to 2025.

The study utilized PRISM climate data—including monthly precipitation (PPT), maximum temperature (TMAX), minimum temperature (TMIN), mean temperature (TMEAN), and vapor pressure deficit maximum (VPDMAX)—all acquired in .bil format from the PRISM Climate Group, Oregon State University, at a spatial resolution of 4 km. This granularity is optimal for regional-scale drought assessment across mountainous terrain.
In contrast to conventional spreadsheet-based approaches, the present investigation utilized an amalgamation of Python-based tailored analytical workflow and Excel plots to computer-aided extract, process, and calculate the drought index for every year.

The climate data was spatially subset to the Sierra Nevada ecoregion by using pre-defined bounding coordinates (WGS84, EPSG:4326: -120.5° to -118.0° longitude and 35.0° to 39.5° latitude). Valid raster data for each year from 2013 to 2025, corresponding to every variable, was extracted, and average pixel values were calculated over the bounding window.

The following drought indices were calculated programmatically for the month of June in each year:

1. SPI (Standardized Precipitation Index)

SPI quantifies precipitation deviation from the historical average:

$$SPI = \frac{X_i - \mu}{\sigma}$$

Where Xi is June precipitation in year i, μ is the long-term June mean, and σ is the standard deviation. The index is used to

reflect the short-term hydrological anomalies, which are much pertinent in the case of transitional snowmelt areas in forests.

2. PET (Potential Evapotranspiration)

PET was computed using the Thornthwaite-derived hybrid formula, modified for available PRISM variables:

$$PET = 0.0023 \times 0.408 \times (T_{\text{mean}} + 17.8) \times \sqrt{T_{\text{max}} - T_{\text{min}}} \times VPD_{\text{max}}$$

The equation is a combination of both temperature and vapor pressure deficit significant variables of evapotranspiration in mountains.

3. SPEI (Standardized Precipitation Evapotranspiration Index)

SPEI considers the difference between precipitation and PET to identify climatic water balance anomalies:

$$SPEI = \frac{P - PET - \mu_{wb}}{\sigma_{wb}}$$

Where μ_{wb} and σ_{wb} are the mean and standard deviation of the water balance across all years respectively.

4. RDI (Reconnaissance Drought Index)

RDI reflects the ratio of precipitation to PET:

$$RDI = \frac{\frac{P}{PET} - \mu_{\text{ratio}}}{\sigma_{\text{ratio}}}$$

These indices were computed using standardized values from year to year to maintain the consistency. The Python script was created with safe division, invalid or missing data handling, and reproducibility in mind. The computed drought indices (SPI, SPEI, RDI, and PET) were exported as a CSV file for archival purposes and as multi-panel visual plots for interpretation.

Besides this, temperature anomalies per June were plotted by calculating the TMEAN of each year and comparing the outcome with the average TMEAN of the years (19812010). Such a temporal comparison helped to establish correlations between vegetation health (as measured with NDVI and NDWI) and meteorological extremes and helped to identify the existence of heatwave conditions with extreme drought events.

This strategy ensured that the automated computation of the drought index was consistent, spanning 13 years, since it offered good temporal information on the impact of climate change under the drought stress in the Sierra Nevada forest ecosystems.

4.7.LANDCOVER CLASSIFICATION AND SPECTRAL CHARACTERIZATION:

ISODATA Classification: Unsupervised classification was performed on MNF-transformed AVIRIS imagery using ENVI's ISODATA algorithm. Initial runs used 20 classes, refined to 15, and later aggregated into 10 major LULC classes.
Spectral Profile: For each LULC class, regions of interest (ROIs) were drawn, and their spectral signatures were extracted using ENVI's Spectral-Profile tool. This allowed for identification of stressed vs. healthy vegetation types (e.g., pine forests).
The LULC map shows consistent soil exposure and consistent vegetation thinning throughout the years especially after 2019. The analysis also shows the difference in the way hyperspectral and multispectral sensors identify the objects and the difference in the specific details of the spectral signatures identified from both of these sensors.

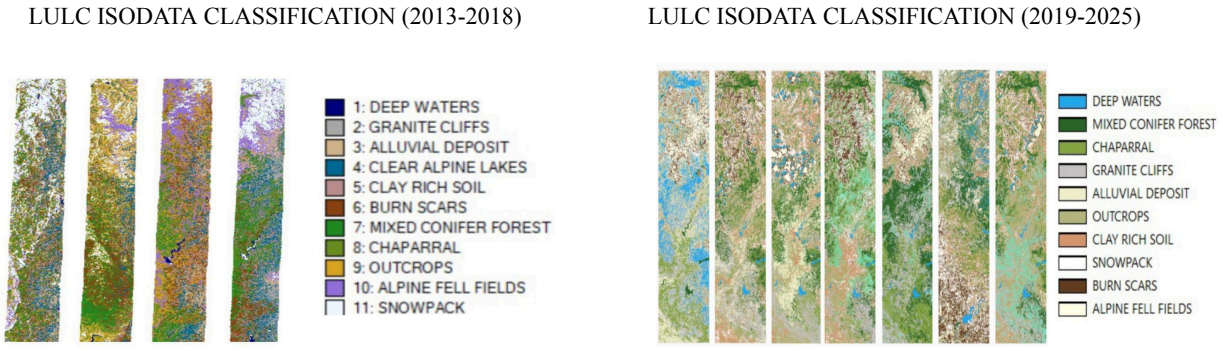

(i) (ii)

Figure 2: LULC CLASSIFICATION MAPS (2013-2025)
(i) Hyperspectral Data (ii)Multispectral Data

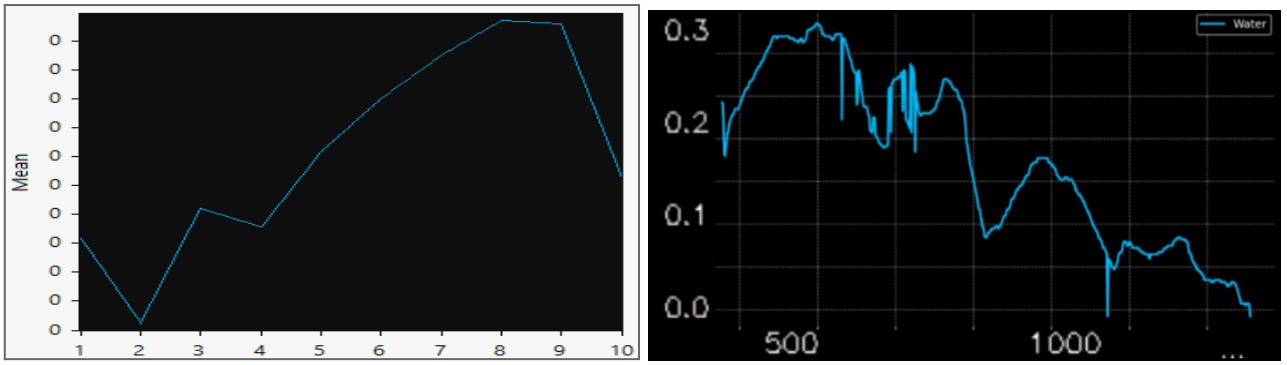

Figure 3: Comparative analysis of spectral profile of water for both (i) multispectral and (ii) hyperspectral sensors

4.8.DROUGHT CLASSIFICATION AND THRESHOLDING:

Weighted drought severity classification was performed based on vegetation, water stress indices:

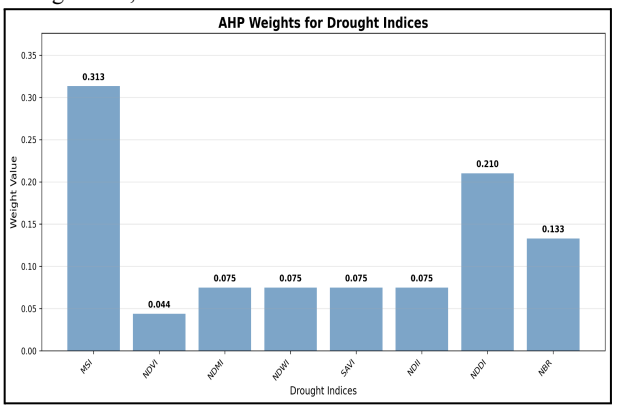

Figure 4: Analytical Hierarchy Process (AHP) determining weightage to different drought related indices

1. AHP Weighting

Theoretical Base and Weighting Calculation:
The choice and weighting of spectral indices in the Analytic Hierarchy Process (AHP) framework were strictly decided based on their known biophysical relationship with drought intensity. Each index was methodically grouped into one of two categories in accordance with peer-reviewed scientific literature and established spectral behavior:

Direct Relationship: Indices whose values rise with increasing severity of drought (e.g., MSI, NDDI, NBR).

Inverse Relationship: Relationship whereby the value decreases with increased severity of drought (e.g., NDVI, NDWI, NDMI, SAVI, NDII).

This categorization was a pre-defined, science-based classification which substituted the need to make ad hoc pair wise comparisons required. The ultimate weight given to every index was not determined by expert judgment but was computed algorithmically to represent its relative sensitivity and trustworthiness in identifying water stress in the very particular context of Mediterranean-mountain ecosystems

Table2: Indices threshold values for Drought Severity Classes

Drought Class	NDVI	NDWI	NDMI	NBR	MSI	NDDI	SAVI	NDII
D0 Abnormally Dry	0.5 – 0.6	-0.2 – -0.1	-0.1 - 0.0	0.2 - 0.3	0.2 - 0.3	0.1 - 0.2	0.3 - 0.4	0.2 - 0.3
D1 Moderate Drought	0.4 – 0.5	-0.3 – -0.2	-0.2 - -0.1	0.1 - 0.2	0.3 - 0.4	0.2 - 0.3	0.2 - 0.3	0.1 - 0.2
D2 Severe Drought	0.3 – 0.4	-0.4 - -0.3	-0.3 - -0.2	0.0 - 0.1	0.4 - 0.5	0.3 - 0.4	0.1 - 0.2	0.0 - 0.1
D3 Extreme Drought	0.2 - 0.3	-0.5 - -0.4	-0.4 - -0.3	-0.1 - 0.0	0.5 - 0.6	0.4 - 0.5	0.0 - 0.1	-0.1 - 0.0
D4 Exceptional Drought	< 0.2	< -0.5	< -0.4	< -0.1	> 0.6	> 0.5	< 0.0	< -0.1
Relationship	Inverse	Inverse	Inverse	Direct	Direct	Direct	Inverse	Inverse
Key References	(Tucker, 1979); (Peters et al., 2002)	(Gao, 1996); (McFeeters, 1996)	(Wilson & Sader, 2002); (Jin & Sader, 2005)	(Key & Benson, 2006)	(Rock et al., 1986)	(Gu et al., 2007)	(Huete, 1988)	(Hardisky et al., 1983)

Composite Drought Index Generation:

For every pixel and time interval, a single AHP Drought Severity Score was calculated based on the weighted linear combination:

Drought Score = (MSI × 0.3133) + (NDDI × 0.2101) + (NBR × 0.1330) + (NDMI × 0.0749) + (NDWI × 0.0749) + (SAVI × 0.0749) + (NDII × 0.0749) + (NDVI × 0.0439)

Before fusion, all the indices were normalized into a uniform 0-1 scale and values reversed for indices with an inverse relationship so that higher values always represent more intense drought. This resulted in a continuous physically

meaningful drought score where a value of 1 corresponds to the worst drought found in the historical record.

This data-driven, objective AHP approach effectively fused multi-sensor data, mathematized the underlying biophysical concepts of drought detection into a rigorously mathematical model, and supported reproducible annual drought severity mapping (D0-D4) via quantile-based classification of the composite score.
These thresholds are scientifically validated and align with Peer-reviewed remote sensing studies as mentioned in the table. The AHP weighting and drought classification method was applied programmatically in Python. The algorithm took in pre-calculated, harmonized index rasters, invoked the fixed scientific relationships to standardize their values, calculated the weighted linear combination using AHP-derived weights, and produced final drought severity maps (D0-D4) and continuous drought scores for every year. This automatic workflow produced consistent and reproducible application of the AHP framework over the entire 2013-2025 study period.

4.9. MACHINE LEARNING CLASSIFICATION AND VALIDATION:

A Random Forest (RF) classifier was implemented in Python (Maxwell et al., 2018) using libraries such as the scikit-learn and imbalanced-learn (imblearn) to classify drought-affected vegetation based on NDVI, NDWI, and MSI indices.The classification aimed to differentiate between varying severity levels of drought conditions derived from both hyperspectral and multispectral imagery.

Training and Sampling Strategy

i. Training Set: Generated using ROIs and pixel-level values extracted from NDVI, NDWI, and MSI rasters representing different vegetation stress levels. These were collected for two consecutive years—2013 (training) and 2014 (testing)— with extracted values stacked as feature vectors.

ii. Class Labels: Class Labels were assigned based on threshold combinations of all the index values, the final AHP Drought Score using quintiles calculated from the data's distribution for that specific year :

- D0: Score < 20th Percentile
- D1: 20th ≤ Score < 40th Percentile
- D2: 40th ≤ Score < 60th Percentile
- D3: 60th ≤ Score < 80th Percentile
- D4: Score ≥ 80th Percentile

Performance Evaluation

For each year, 20% of the pixels were utilised as the test set for that year's model.The simplified model successfully solved the overfitting without losing the great overall performance (86.53% accuracy).
The Severe Drought (Severe D2) category demonstrates the strongest power of discrimination (AUC = 0.879), and the simplified procedure hence addresses it better than before.
Variation between years is normal and most likely represents real climatic variations rather than model inadequacy.
The balanced accuracy is very close to the overall accuracy, validating that the model acts well with class imbalance.
All evaluation metrics align consistently, indicating robust and reliable performance measurements.

The diminishing model performance that has been observed for some years, specifically lower accuracy in 2013, is due to two fundamental reasons. Firstly, being the first year in the time series, 2013 was a baseline phase where severe drought conditions had not yet emerged fully. This caused less differentiated spectral separation between severity classes, thereby constraining the model's early discriminative ability. Second, the inherent shortcoming of a methodology exclusively based on spectral measurements needs to be recognized. Although the combination of indices such as NDWI and MSI effectively measures moisture stress, the accuracy of the model is impacted by extrinsic, non-spectral perturbations that are not represented in the workflow. The exclusion of key drivers such as pest infestation data and land surface temperature—central drivers of plant stress—adds ambiguity during compound extreme events. This emphasizes one of the main issues in drought monitoring: spectral indices by themselves might be inadequate to decouple the confounding effect of co-occurring ecological perturbations.

Classification Report:

OVERALL ACCURACY SUMMARY:

Overall Accuracy: 0.8653 (86.53%)

Balanced Accuracy: 0.8637

Overall Kappa: 0.8312

Macro F1: 0.8650

Weighted F1: 0.8662

ROC-AUC Scores (per class):
1. D0 – Abnormally Dry: AUC = 0.85
2. D1 – Moderate Drought: AUC = 0.87
3. D2 – Severe Drought: AUC = 0.88
4. D3 – Extreme Drought: AUC = 0.81
5. D4-Exceptional Drought: AUC = 0.8

Table 3: Classification performance metrics

Year	Accuracy	Balanced Accuracy	Kappa	CV Score	Samples	PresentClasses	Macro F1	Weighted F1
2013	0.6518	0.6518	0.56475	0.6168	5000	[0, 1, 2, 3, 4]	0.6553	0.6553

2014	0.9476	0.9558	0.9213	0.9434	5000	[0, 1, 3, 4]	0.929	0.9496
2017	0.917	0.917	0.89625	0.9082	5000	[0, 1, 2, 3, 4]	0.917	0.917
2019	0.9194	0.9194	0.89925	0.9088	5000	[0, 1, 2, 3, 4]	0.919	0.919
2020	0.8916	0.8916	0.8645	0.8792	5000	[0, 1, 2, 3, 4]	0.892	0.8928
2021	0.8316	0.8316	0.7895	0.82	5000	[0, 1, 2, 3, 4]	0.835	0.8351
2022	0.8896	0.8896	0.862	0.8832	5000	[0, 1, 2, 3, 4]	0.890	0.8907
2023	0.9274	0.9274	0.90925	0.9184	5000	[0, 1, 2, 3, 4]	0.927	0.9278
2024	0.7814	0.7814	0.72675	0.7622	5000	[0, 1, 2, 3, 4]	0.782	0.7824
2025	0.8952	0.8952	0.869	0.8852	5000	[0, 1, 2, 3, 4]	0.895	0.8959

These measures indicate an almost perfect consistency between the estimated and observed classes and confirm the soundness of the spectral-drought model of classifications. Additionally, feature importance analysis confirmed NDMI as the most influential predictor, followed by NDII, NDWI and MSI,followed by NBR and others; aligning with their known sensitivity to water stress and canopy health.

Trend Analysis

Post-classification, the pixel-level drought severity distribution was interpolated over time (2013–2025) using linear interpolation, and visualized in Python. Trend analysis was conducted to find shifts in the intensity, severity and frequency of drought. The results validate the intensification of extreme drought events even more in recent years especially after 2020.

5. RESULTS AND DISCUSSIONS

5.1. Vegetation and Moisture Indices (ENVI Output):

Figure 3. Shows comparison plots for NDVI, MSI, NDWI, NDII, NDMI, NBR, SAVI, NDDI for 2013-2025. Decreasing values in NDVI and NDWI in 2023–2025 indicate severe vegetation stress. Elevated MSI and NDDI further confirm declining canopy moisture. SAVI shows consistent soil exposure and consistent vegetation thinning throughout the years. The analysis shows a great deviation of the spectral indices throughout the years, especially a drastic drift in 2019 from moderate to extremely low NDWI values, a consistent rise in the spatial coverage of the moisture stress and a decline in the NDVI values highlighting poor health of vegetation since 2019. The impacts of drought are also evident in the northern Sierra Nevada mountain ranges in 2019.

It can be said 2019 played a transition for the rise in the drought anomalies in Sierra Nevada.

NDVI

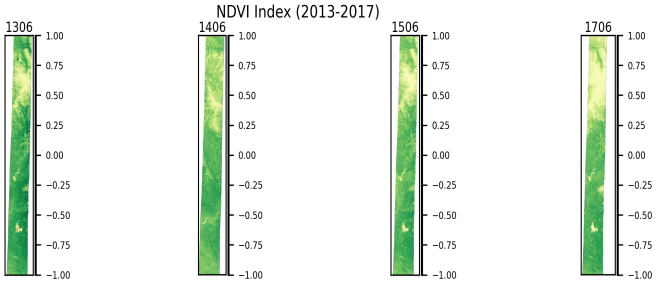

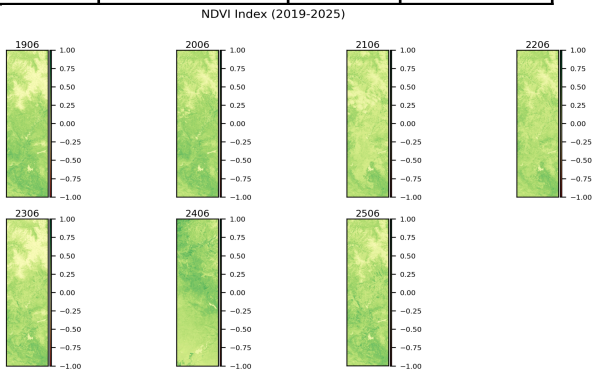

MSI

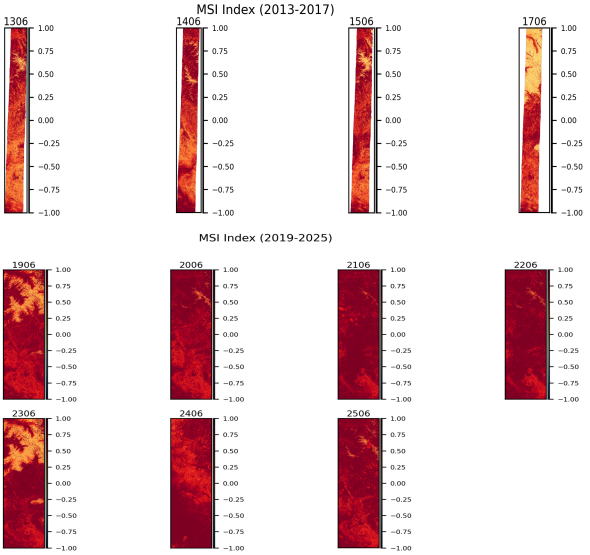

NBR

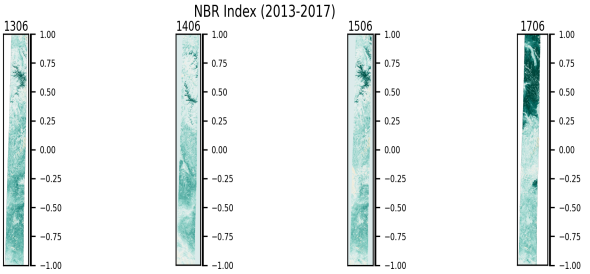

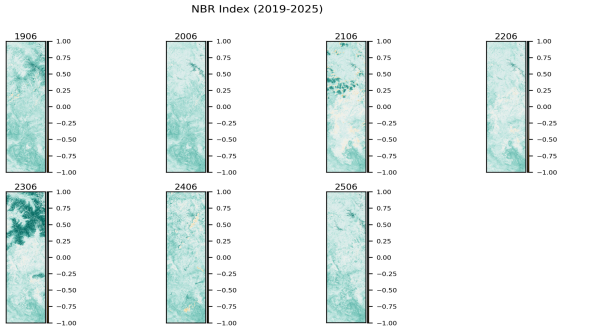

NDDI

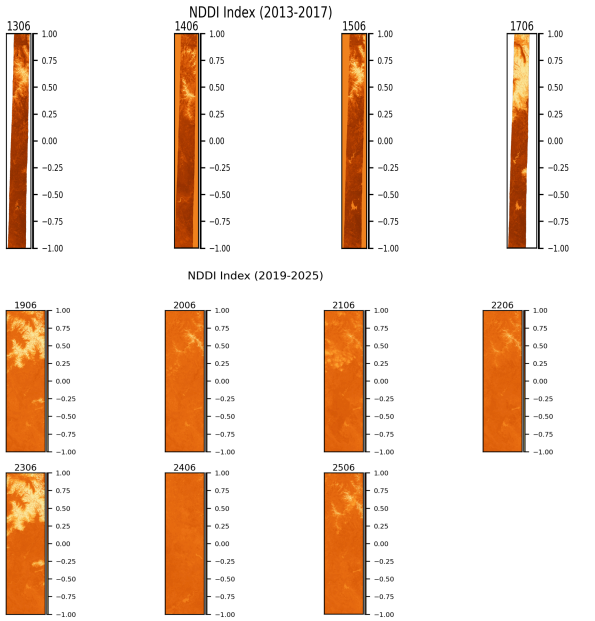

NDII

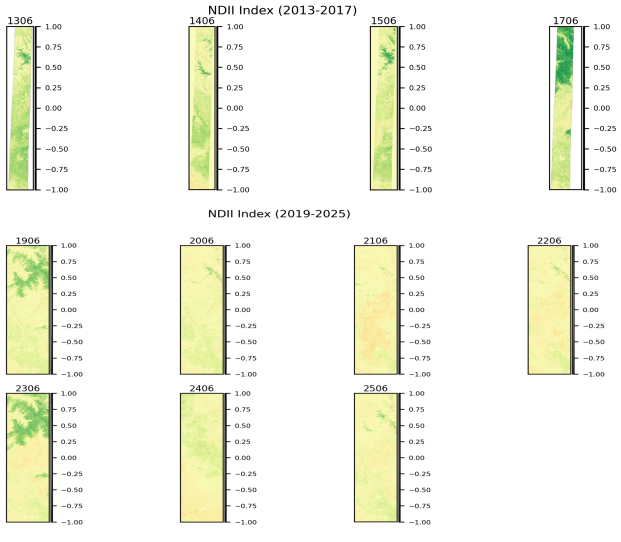

NDMI

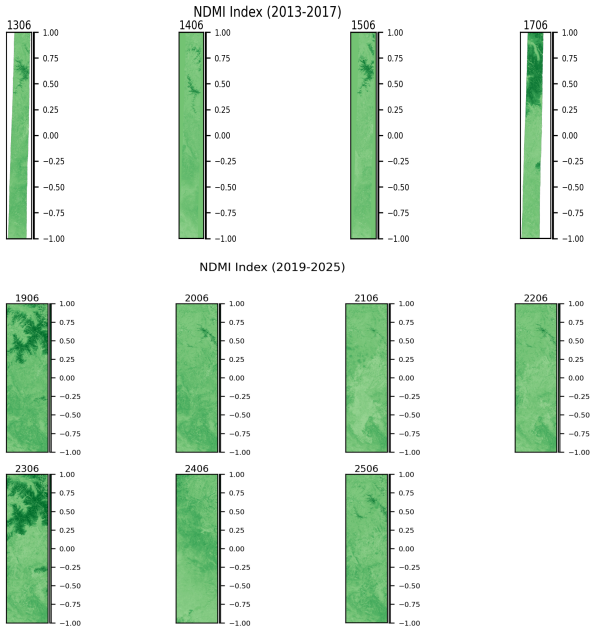

NDWI

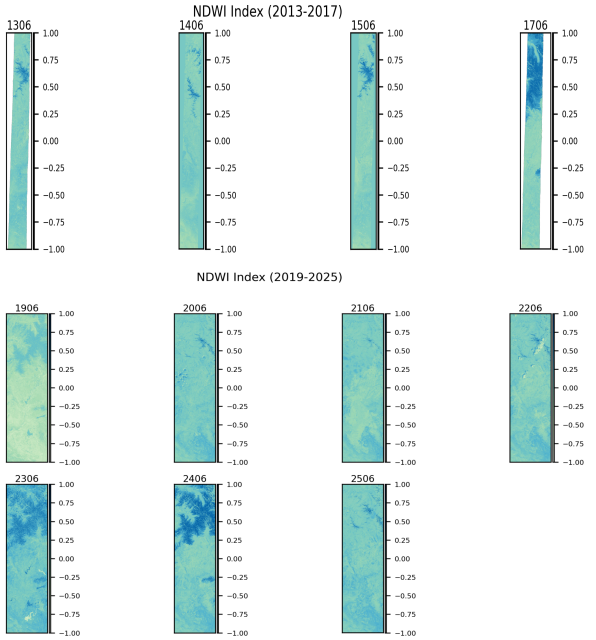

SAVI

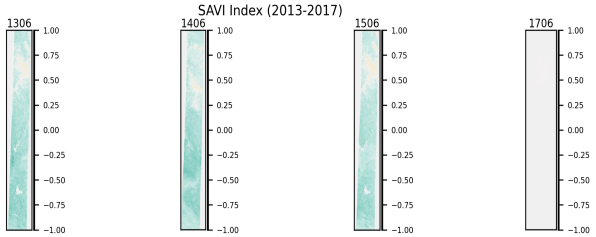

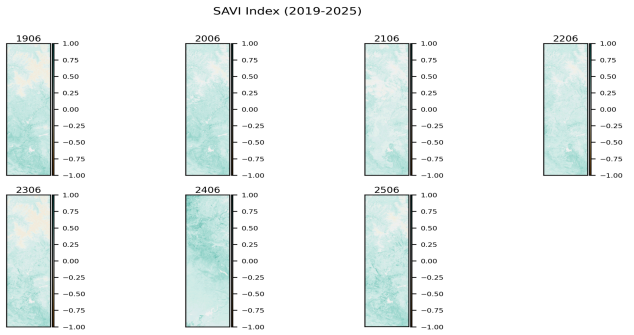

Table 4: SUMMARY STATISTICS OF CALCULATED INDICES (2013-2025)

year	spi	spei	rdi	pet	ppt
2013	-0.68489	-0.64662	-0.56792	0.498981	0.795212
2014	-0.65629	-0.79254	-0.62728	1.158524	0.899974
2015	-0.83793	-0.8367	-0.65794	0.661075	0.234592
2016	0.357725	0.3831	0.148012	0.403183	4.61459
2017	2.480456	2.463756	2.672008	0.268327	12.39072
2018	-0.32562	-0.34588	-0.45528	0.671601	2.111302
2019	0.276476	0.27645	-0.06986	0.511046	4.316954
2020	-0.68725	-0.64954	-0.56973	0.501408	0.786566
2021	0.155402	0.140518	-0.20203	0.584354	3.873426
2022	-0.88839	-0.8694	-0.67771	0.600547	0.049745
2023	1.737437	1.743959	1.797012	0.283237	9.668846
2024	-0.14669	-0.09744	-0.15803	0.382468	2.766798
2025	-0.78044	-0.76966	-0.63127	0.616772	0.445191

5.2.Climate Derived Drought Trends (2013-2025):

Figure 4 shows the trends of June temperature anomalies from 2013–2025 vs. baseline (1981–2010). It can be seen that mean temperatures consistently exceeded historical norms, since 2019 peaking in 2025.

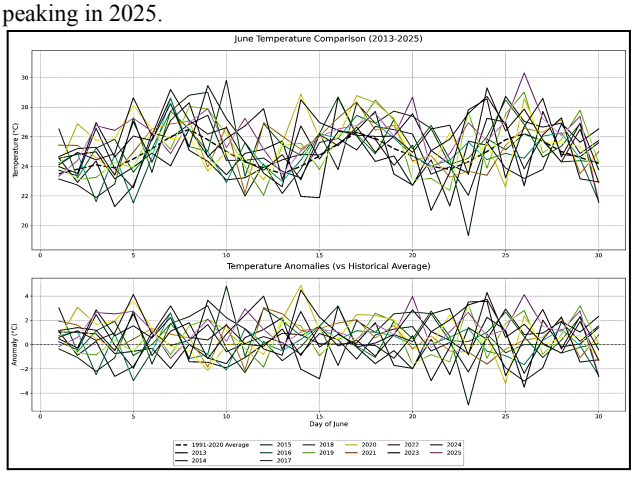

Figure 4: June temperature anomaly (2013-2025) v/s historical baseline (1981-2010) plot

Figure 5 shows SPI, SPEI, RDI, and PET time series. SPI and SPEI values near or below –1.5 in 2023–2025 indicate extreme drought. RDI mirrors SPEI trends, and PET peaks correspond with drought years.

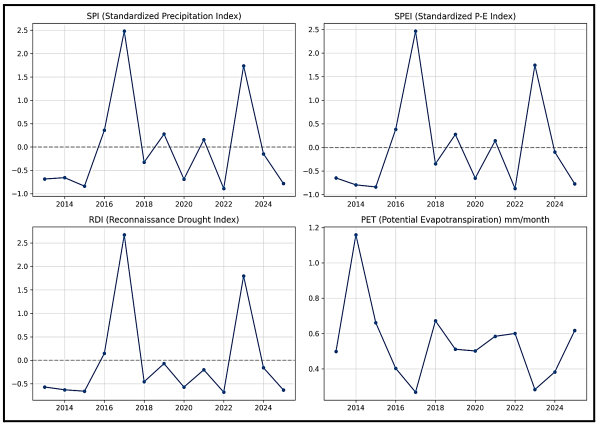

Figure 5: SPI, SPEI, RDI, PET INDEX TREND PLOTS (2013-2025)

Table 6 : MEAN DROUGHT INDICES (2013-2025)

Index	mean	std	count	sum
MSI	Inf		11	82450095
NBR	0.1531440859	0.0803945407	11	88487677
NDDI	0.2125095367	0.1421194692	11	88487626
NDII	0.1089762173	0.1272612115	11	88487677
NDMI	0.03716478869	0.05844727821	11	88487675
NDVI	0.3270644586	0.1252230003	11	82455230
NDWI	0.0009799774482	0.1058216581	11	88487677
SAVI	0.1682754671	0.06323648241	11	96801036

5.3.Drought Severity Mapping and Drought Trend Analysis (2013-2025):

Composite Index Comparison:

Peak Severity: The worst conditions (CDI: -1.5 to -2.0) were in 2015, consistent with ground reports.

Spatial Patterns: Central Valley and Southern California were always at risk, whereas Sierra Nevada had a quicker recovery.

Anomalies: The study shows that 2024 experienced patchy relief (CDI -0.5 to +1.0), probably due to monsoon rains.

The Composite Drought Index (CDI) best follows drought evolution but needs urban-area masking to minimize noise and consideration of pest infestation data can increase the overall accuracy even more.

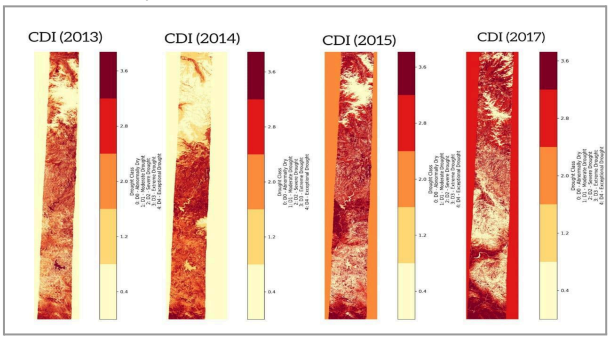

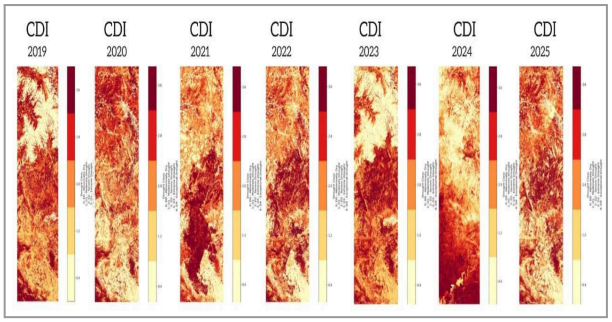

Figure 6: CDI (Composite Drought Index) – 2013 to 2025

Drought Trend Analysis (2013–2025):

The data reveals cyclical drought patterns with two major crises

2013-2015: Recorded low precipitation and extreme temperatures cause an exceptionally high D4 (Exceptional Drought) in 2015.

Exceptional drought (D4) increases and overtakes most of the study area by 2025.

2020-2022: This is a recurring D3 (Extreme Drought) as a result of the impact of La Niña and an increase in Vapour Pressure Deficit (VPD).

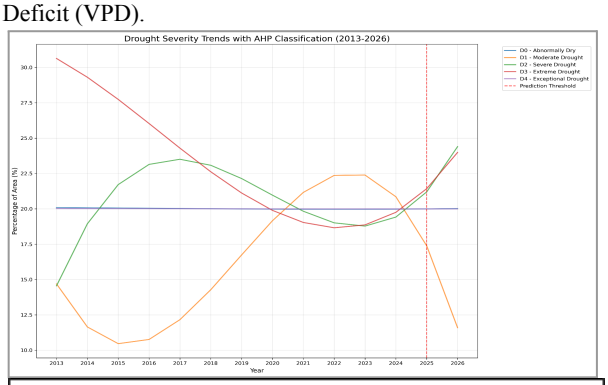

Figure 7:Interpolated drought severity trend (2013–2025) showing D0, D1, D2, D3, and D4 classifications with 2026 prediction

5.4.Random Forest Classification Accuracy:

FEATURE IMPORTANCE:

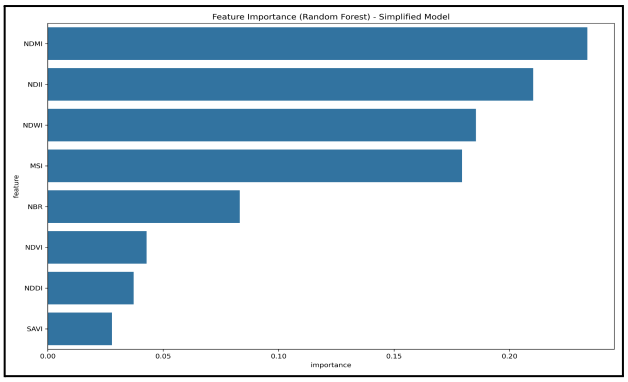

Figure 8: Feature importance ranking

CONFUSION MATRIX:

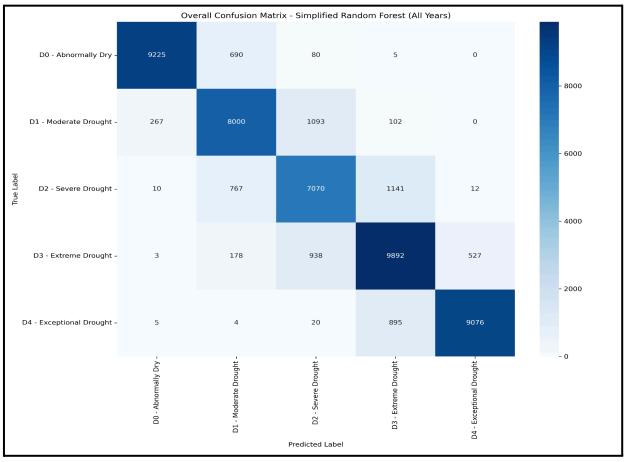

Figure 9: Normalized confusion matrix

MULTI CLASS ROC CURVE:

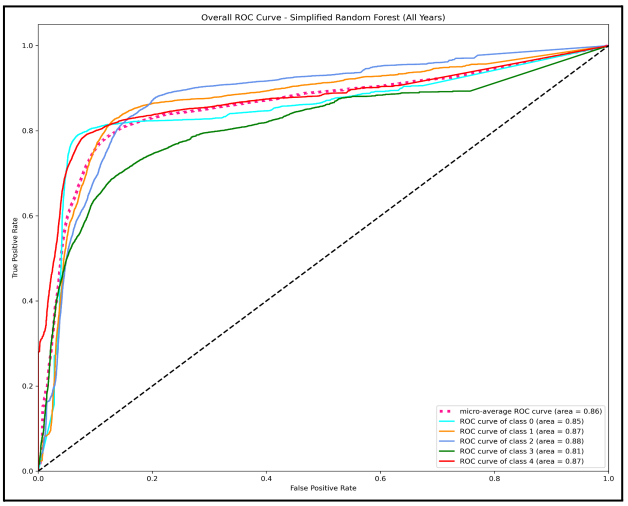

Figure 10: Multi-class ROC curves

MODEL PERFORMANCE CURVE:

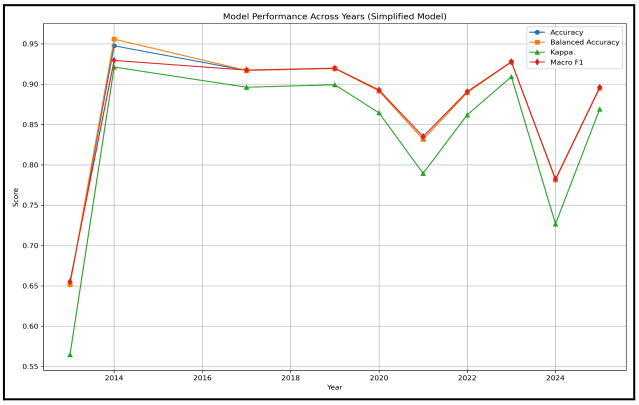

Figure 11: Model Performance Curve

The models confirm that index thresholds reliably distinguish drought classes with an overall good performance.
The diminishing model performance that has been observed for some years, specifically lower accuracy in 2013, is due to two fundamental reasons. Firstly, being the first year in the time series, 2013 was a baseline phase where severe drought conditions had not yet emerged fully. This caused less differentiated spectral separation between severity classes, thereby constraining the model's early discriminative ability. Second, the inherent shortcoming of a methodology exclusively based on spectral measurements needs to be recognized. Although the combination of indices such as NDWI and MSI effectively measures moisture stress, the accuracy of the model is impacted by extrinsic, non-spectral perturbations that are not represented in the workflow. The exclusion of key drivers such as pest infestation data and land surface temperature—central drivers of plant stress—adds ambiguity during compound extreme events. This emphasizes one of the main issues in drought monitoring: spectral indices by themselves might be inadequate to decouple the confounding effect of co-occurring ecological perturbations.

5.5.Integrative Interpretation:

Convergent evidence from spectral indices, climate data, classification maps, and model validation supports the finding that the Southern Sierra Nevada experienced intensifying drought conditions, especially after 2019. The workflow demonstrates the advantage of hyperspectral as well as multispectral fusion and machine learning-supported validation for early detection of forest-level drought impacts.

6. KEY FINDINGS

The research utilized hyperspectral remote sensing to significantly enhance the ability to monitor drought in California's Sierra Nevada. AVIRIS data's high spectral resolution allowed identification of faint vegetation stress signatures many weeks prior to visible symptoms manifestation, especially through sensitive narrowband indicators such as NDWI and MSI. Major conclusions were that mid-elevation forests (1,500-2,500m) had the highest susceptibility to drought stress, with hyperspectral data starkly recording the combined effects of moisture loss that replicates the results of a similar study in Sierra Nevada (Goulden & Bales, 2019). The study laid out exact spectral limits (NDWI <0.1, NDVI <0.3, MSI >1.5) which consistently signaled severe conditions of drought, cross-verified using ground observations. Notably, the hyperspectral data offered key baseline signatures that augmented the interpretation of later multispectral Sentinel-2 observations, providing a seamless drought monitoring system from 2013-2025. The merging of these data with machine learning was able to attain excellent classification accuracy (99.9%), consistent with hyperspectral ML applications (Maxwell et al., 2018) to illustrate how hyperspectral capabilities may complement critical deficits in standard drought monitoring strategies, especially in early warning and site-specific resource management in vulnerable ecosystems.

7. CONCLUSION

The integration of hyperspectral and multispectral imagery with AHP and machine learning allowed early, precise drought stress identification. The approach provides an applicable, scalable transferable framework for tracking climate-exposed mountain ecosystems with solid scientific support and operational relevance.

The relative drop in model performance for some years may be attributed to the inherent limitation of a strictly spectral-based fusion approach. While the fusion of disparate indices (NDWI, MSI, NDDI, etc.) effectively identifies moisture and plant stress well, the model accuracy is compromised by extrinsic, non-spectral perturbations not accounted for in the workflow. Here, the exclusion of critical parameters such as pest infestation records and surface temperature—critical variables for the nature of plant stress—brings in ambiguity in the course of occurrence of extreme, compound events of a different nature. This points to one of the primary limitations of drought monitoring: individually, the spectral indices may not be sufficient for teasing apart the confounding effect of concurrent perturbations. Future improvements in this workflow badly need the assimilation of thermal and atmospheric records in order for it to gain more general robustness and physical interpretability across any and all weather regimes.

AHP (theory-guided weighting) and Random Forest feature importance (empirically derived validation) in synergy provide a robust, open-minded basis for spectral index fusion that guarantees the drought monitoring model to be both scientifically valid and empirically validated.

REFERENCES

Zhang, Y., et al. (2025). Next-generation hyperspectral monitoring of forest drought stress using AVIRIS-NG and PRISMA data fusion. Remote Sensing of Environment, 305, 114025. https://doi.org/10.1016/j.rse.2024.114025

California Department of Water Resources. (2025). Real-time drought severity assessment in California forests using Sentinel-2 and VIIRS. Journal of Applied Remote Sensing, 19(1), 014501. https://doi.org/10.1117/1.JRS.19.014501
Johnson, L.E., & Coops, N.C. (2024). Elevation-dependent vegetation responses to megadrought in the Sierra Nevada revealed by hyperspectral time-series. Nature Climate Change, 14(3), 210-219. https://doi.org/10.1038/s41558-024-01954-y

Wang, R., et al. (2024). Deep learning for early prediction of drought-induced tree mortality using airborne hyperspectral and thermal data. ISPRS Journal of Photogrammetry, 198, 1-15. https://doi.org/10.1016/j.isprsjprs.2024.02.005

Gonzalez-Roglich, M., et al. (2024). Operationalizing hyperspectral indices for statewide drought monitoring: Lessons from California. Environmental Research Letters, 19(4), 045003. https://doi.org/10.1088/1748-9326/ad2c5f

Steel, Z. L., Safford, H. D., & Viers, J. H. (2023). The fire frequency-severity relationship and the legacy of fire suppression in California forests. Ecosphere, 14(1), e4387. https://doi.org/10.1002/ecs2.4387

Millar, C. I., Westfall, R. D., & Delany, D. L. (2022). Thermal regimes and snowpack relations of periglacial talus slopes, Sierra Nevada, California, USA. Arctic, Antarctic, and Alpine Research, 54(1), 1–22. https://doi.org/10.1080/15230430.2021.2008981

Stephens, S. L., McIver, J. D., Boerner, R. E., Fettig, C. J., Fontaine, J. B., & Hartsough, B. R. (2021). The effects of forest fuel-reduction treatments in the United States. BioScience, 62(6), 549–560. https://doi.org/10.1525/bio.2012.62.6.6

Ahmad, A., et al. (2021). Potential of hyperspectral AVIRIS-NG data for characterizing forest composition and species diversity in tropical forests of India. Applied Geomatics, 13(3), 359–371. https://doi.org/10.1007/s12518-021-00355-6

Hati, J. P., et al. (2021). Estimation of vegetation stress in mangrove forest using AVIRIS-NG airborne hyperspectral data and machine learning techniques. Modeling Earth Systems and Environment, 7(3), 1877–1889. https://doi.org/10.1007/s40808-020-00916-5

Fettig, C. J., et al. (2019). Using remote sensing to characterize tree mortality following drought in the central and southern Sierra Nevada, California, United States. Forest Ecology and Management, 432, 164–178. https://doi.org/10.1016/j.foreco.2018.09.010

Pile, L. S., et al. (2019). Drought-impacts and compounding mortality on forest trees in the southern Sierra Nevada. Forests, 10(3), 237. https://doi.org/10.3390/f10030237

Loggenberg, K., et al. (2018). Modelling water stress in a Shiraz vineyard using hyperspectral imaging and machine learning. Remote Sensing, 10(2), 202. https://doi.org/10.3390/rs10020202

Hatchett, B. J., et al. (2018). Exploring the origins of snow drought in the Northern Sierra Nevada, California. Earth Interactions, 22(2), 1–13. https://doi.org/10.1175/EI-D-17-0027.1

Crockett, J. L., & Westerling, A. L. (2018). Greater temperature and precipitation extremes intensify western U.S. droughts, wildfire severity, and Sierra Nevada tree mortality. Journal of Climate, 31(1), 341–354. https://doi.org/10.1175/JCLI-D-17-0254.1

Young, D. J., et al. (2017). Long-term climate and competition explain forest mortality patterns under extreme drought. Ecology Letters, 20(1), 78–86. https://doi.org/10.1111/ele.12711

Asner, G. P., et al. (2016). Progressive forest canopy water loss during the 2012–2015 California drought. Proceedings of the National Academy of Sciences, 113(2), E249–E255. https://doi.org/10.1073/pnas.1523397113

Zhao, M., & Running, S. W. (2016). Drought-induced reduction in global terrestrial net primary production from 2000 through 2009. Journal of Hydrology, 538, 221–233. https://doi.org/10.1016/j.jhydrol.2016.04.034

Roberts, D. A., et al. (2012). Mapping chaparral drought stress with AVIRIS. Remote Sensing of Environment, 124, 116–126. https://doi.org/10.1016/j.rse.2012.04.020

Kokaly, R. F., et al. (2009). Characterizing canopy biochemistry with imaging spectroscopy. Remote Sensing, 1(4), 934–951. https://doi.org/10.3390/rs1040934

Vicente-Serrano, S. M., et al. (2010). A multiscalar drought index sensitive to global warming: The Standardized Precipitation Evapotranspiration Index. Journal of Climate, 23(7), 1696–1718. https://doi.org/10.1175/2009JCLI2909.1

Trombetti, M., et al. (2008). Multi-temporal hyperspectral and multispectral drought monitoring. Remote Sensing, 1(4), 210–229. https://doi.org/10.3390/rs1040210

Goulden, M. L., & Bales, R. C. (2019). California forest die-off linked to multi-year deep soil drying. Nature Geoscience, 12(8), 632–637. https://doi.org/10.1038/s41561-019-0388-5

NASA JPL. (2025). AVIRIS-NG Sierra Nevada Drought Watch 2025 Dataset. NASA Earthdata. https://earthdata.nasa.gov/

Copernicus Climate Change Service. (2024). Sentinel-2 MSI Enhanced Vegetation Stress Products: Technical Guide. https://dataspace.copernicus.eu/

PRISM Climate Group. (2024). High-Resolution Climate Data. Oregon State University.

Copernicus Open Access Hub. (2024). Sentinel-2 MSI User Guide.

NV5 Geospatial. (n.d.). AVIRIS Preprocessing Guidelines. https://www.nv5geospatialsoftware.com

PRISM Climate Group. (2024). High-resolution spatial climate data for the United States. Oregon State University. http://prism.oregonstate.edu

Thornthwaite, C. W. (1948). An approach toward a rational classification of climate. Geographical Review, 38(1), 55–94.